Inhibition of TNF receptor 1 internalization by adenovirus 14.7K as a novel immune escape mechanism

Wulf Schneider-Brachert,[1] Vladimir Tchikov,[2] Oliver Merkel,[1] Marten Jakob,[2] Cora Hallas,[2] Marie-Luise Kruse,[3] Peter Groitl,[1] Alexander Lehn,[1] Eberhard Hildt,[4] Janka Held-Feindt,[5] Thomas Dobner,[1] Dieter Kabelitz,[2] Martin Krönke,[6] and Stefan Schütze[2]

[1]Institute for Medical Microbiology and Hygiene, University of Regensburg, Regensburg, Germany. [2]Institute of Immunology and [3]Department of Internal Medicine, University Hospital of Schleswig-Holstein, Campus Kiel, Kiel, Germany. [4]Department of Medicine II, University of Freiburg, Freiburg, Germany. [5]Department of Neurosurgery, University Hospital of Schleswig-Holstein, Campus Kiel, Kiel, Germany. [6]Institute for Medical Microbiology, Immunology, and Hygiene, Center of Molecular Medicine Cologne, University of Cologne, Cologne, Germany.

The adenoviral protein E3-14.7K (14.7K) is an inhibitor of TNF-induced apoptosis, but the molecular mechanism underlying this protective effect has not yet been explained exhaustively. TNF-mediated apoptosis is initiated by ligand-induced recruitment of TNF receptor–associated death domain (TRADD), Fas-associated death domain (FADD), and caspase-8 to the death domain of TNF receptor 1 (TNFR1), thereby establishing the death-inducing signaling complex (DISC). Here we report that adenovirus 14.7K protein inhibits ligand-induced TNFR1 internalization. Analysis of purified magnetically labeled TNFR1 complexes from murine and human cells stably transduced with 14.7K revealed that prevention of TNFR1 internalization resulted in inhibition of DISC formation. In contrast, 14.7K did not affect TNF-induced NF-κB activation via recruitment of receptor-interacting protein 1 (RIP-1) and TNF receptor–associated factor 2 (TRAF-2). Inhibition of endocytosis by 14.7K was effected by failure of coordinated temporal and spatial assembly of essential components of the endocytic machinery such as Rab5 and dynamin 2 at the site of the activated TNFR1. Furthermore, we found that the same TNF defense mechanisms were instrumental in protecting wild-type adenovirus–infected human cells expressing 14.7K. This study describes a new molecular mechanism implemented by a virus to escape immunosurveillance by selectively targeting TNFR1 endocytosis to prevent TNF-induced DISC formation.

Introduction

During coevolution with the human immune system, viruses have adapted sophisticated strategies to escape the defense mechanisms of the infected host (reviewed in refs. 1, 2). Early region 3 (E3) of human adenoviruses encodes several genes to outwit TNF receptor–mediated eradication to ensure production of high yields of viral progeny (3–6). Among these, E3-14.7K (14.7K) is a potent inhibitor of TNF-mediated cytotoxicity (7–9). Although several proteins interacting with 14.7K have been identified, the molecular mechanism of prevention of apoptosis by 14.7K still remains enigmatic (10). Ligand-bound TNF receptor 1 (TNFR1) is internalized within minutes via clathrin-coated vesicles (CCVs) (11), but the functional contribution of receptor endocytosis to activation of the pleiotropic TNF signaling pathways is still under investigation (12). Accumulating evidence suggests that signaling complexes derived from activated cell-surface receptors are still in their active state in endosomes, and certain signaling events appear to require endocytosis for full activation to occur (13, 14). As we have shown previously, pharmacological inhibition of TNFR1 internalization prevents TNF-mediated apoptosis (15). Furthermore, we recently identified a distinct domain within the cytoplasmic sequence of TNFR1 responsible for mediating receptor endocytosis and demonstrated that TNFR1 internalization and death-inducing signaling complex (DISC) formation are inseparable events (16). In addition, the molecular mechanisms orchestrating DISC formation in TNFR1 apoptosis signaling are largely unknown (16–18). These findings prompted us to investigate the potential involvement of TNFR1 endocytosis in 14.7K-mediated inhibition of TNF-induced apoptosis.

Results

Murine fibroblast cell lines NIH 3T3 and C127 were infected with recombinant retroviruses expressing either wild-type 14.7K (14.7K) or a previously described loss-of-function mutant of the 14.7K protein containing a cysteine residue replaced by serine (designated PM-14.7K in the present study) (19). Treatment of PM-14.7K NIH 3T3 and PM-14.7K C127 cells with TNF in the presence of cycloheximide (CHX) revealed dose-dependent cell death, determined by crystal violet staining, whereas NIH 3T3 and C127 cells expressing 14.7K were protected from TNF-triggered cytotoxicity (data not shown). These results were confirmed by FACS analysis using FITC-coupled annexin V to determine TNF-induced apoptosis (Figure 1, A–D). PM-14.7K NIH 3T3 and PM-14.7K C127 cells revealed increased annexin V staining following TNF/CHX treatment, indicative of typical apoptotic changes in membrane biochemistry (Figure 1, A and C). In contrast, NIH 3T3 and C127 cells expressing 14.7K did not show significant annexin V binding after incubation with TNF/CHX compared with TNF treatment alone (Figure 1, B and D). Thus, 14.7K protects NIH 3T3 and C127 cells from TNF-induced apoptosis.

Nonstandard abbreviations used: Ad5, adenovirus 5; CCP, clathrin-coated pit; CCV, clathrin-coated vesicle; CHX, cycloheximide; DD, death domain; DISC, death-inducing signaling complex; E3, early region 3; FADD, Fas-associated death domain; 14.7K, E3-14.7K; RIP-1, receptor-interacting protein 1; TNFR1, TNF receptor 1; TRADD, TNF receptor–associated death domain; TRAF-2; TNF receptor–associated factor 2.

Conflict of interest: The authors have declared that no conflict of interest exists.

Citation for this article: *J. Clin. Invest.* **116**:2901–2913 (2006). doi:10.1172/JCI23771.

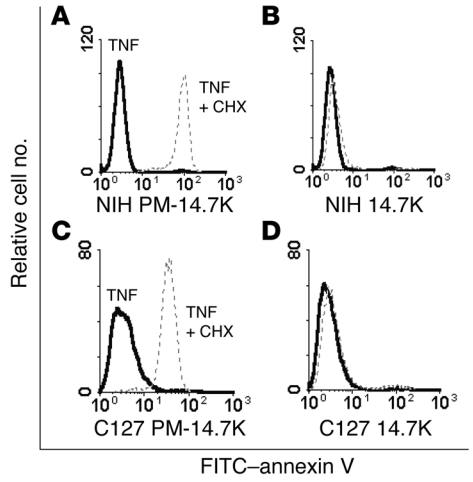

Figure 1
14.7K protects NIH 3T3 cells from TNF-induced apoptosis. NIH 3T3 and C127 cells expressing either PM-14.7K (**A** and **C**) or 14.7K (**B** and **D**) were treated with 100 ng/ml TNF for 18 hours in the absence (bold lines) or presence of 12.5 μg/ml CHX (dotted lines). TNF-induced apoptosis was monitored by FITC–annexin V staining using FACS analysis.

TNFR1-mediated apoptosis is induced by ligand-triggered recruitment of adaptor proteins to the death domain (DD) through shared protein motifs (20). Therefore, we determined whether efficient DISC formation by recruitment of TNF receptor–associated death domain (TRADD), Fas-associated death domain (FADD), and caspase-8 was affected in 14.7K cells. Several recent studies have failed to demonstrate the existence of a TNFR1-associated DISC using immunoprecipitation (17, 18), pointing to a difference between efficient DISC formation in TNF signaling and other apoptosis signaling receptors, such as CD95 (21) or TNF-related apoptosis-inducing ligand receptor 1 (TRAIL-R1) and TRAIL-R2 (22). These observations suggest that TNFR1 apoptosis signaling is regulated by a specific, but still poorly defined, mechanism (12, 23). To address this problem, we developed a new technique for purification of morphologically intact endocytic vesicles harboring magnetically labeled TNFR1 complexes using a custom-made high-gradient magnetic chamber (16). Magnetic labeling was performed using biologically active biotin-TNF as a ligand coupled to magnetic streptavidin microbeads, as recently described. After gentle mechanical homogenization, morphologically intact vesicles containing activated TNF–TNF receptor complexes were isolated in the magnetic chamber. In magnetic TNFR1 fractions isolated from PM-14.7K NIH 3T3 cells, TRADD, FADD, and caspase-8 were scarcely detectable after preincubation with labeled TNF at 4°C, indicating that receptor clustering on the cell surface by itself is not sufficient for efficient DISC formation (lane 0 min in Figure 2A). After inducing receptor internalization by increasing the temperature to 37°C, rapid recruitment of TRADD, FADD, and caspase-8 was observed in magnetic TNFR1 fractions isolated after 3, 30, and 60 minutes (Figure 2A). Notably, only the 43-kDa caspase-8 was recruited to the DD of TNFR1, pointing to rapid autocatalytic cleavage of the TNFR1-associated 55-kDa procaspase-8 (Figure 2A). Furthermore, after 1 hour the DISC was still attached to the internalized TNFR1, indicating continuous apoptotic signaling from an endosome-derived compartment. Similar results were obtained with magnetic TNFR1 fractions isolated from PM-14.7K C127 cells (Figure 2C). In contrast, TRADD, FADD, and caspase-8 were not detected in magnetic TNFR1 fractions isolated from 14.7K NIH 3T3 cells, even after 1 hour incubation at 37°C, indicating complete inhibition of DISC formation (Figure 2B). This observation was confirmed in 14.7K C127 cells (Figure 2D). Equal loading of proteins was demonstrated by deter-

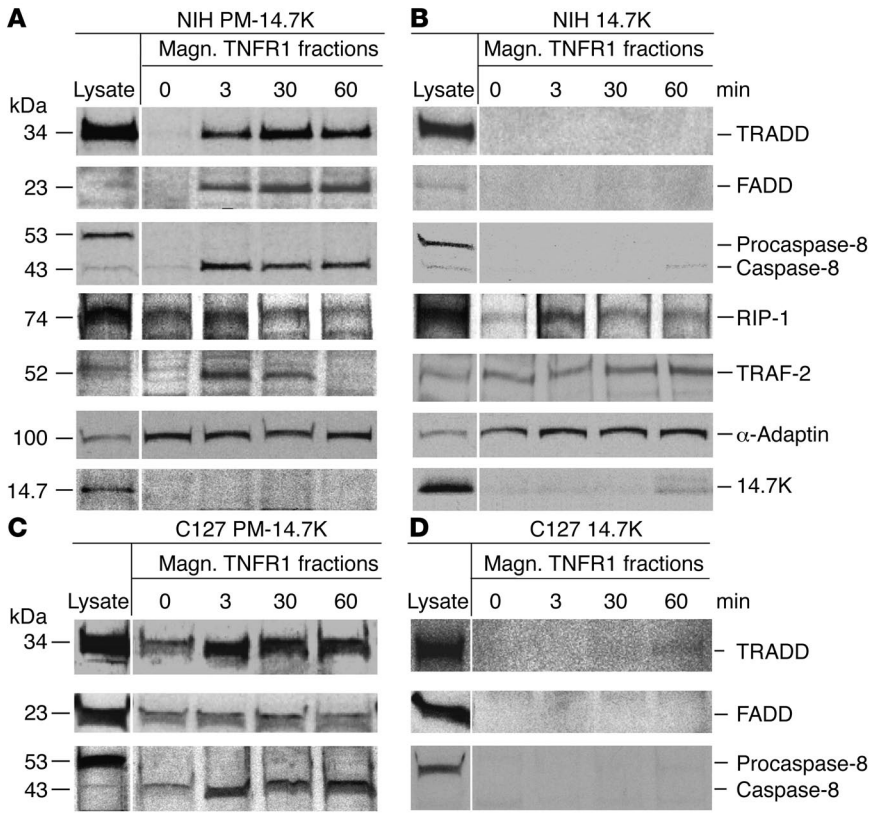

Figure 2
14.7K inhibits DISC assembly in NIH 3T3 and C127 cells. Magnetic fractions harboring labeled TNF-TNFR1 complexes were purified from PM-14.7K and 14.7K cells and immunoblotted with the antibodies indicated. Cellular protein extracts were used as expression controls (lysate). Magnetic (Magn.) TNFR1 fractions purified from NIH 3T3 (NIH) PM-14.7K cells demonstrate TNF-triggered recruitment of TRADD, FADD, and caspase-8 (**A**), whereas TNF treatment failed to induce the TNFR1-associated DISC in the corresponding magnetic fractions isolated from NIH 3T3 14.7K cells (**B**). TNF-dependent recruitment of TRADD, FADD, and caspase-8 to TNFR1 was also demonstrated in PM-14.7K C127 cells (**C**), while 14.7K C127 cells revealed a complete lack of DISC components after TNF treatment (**D**).

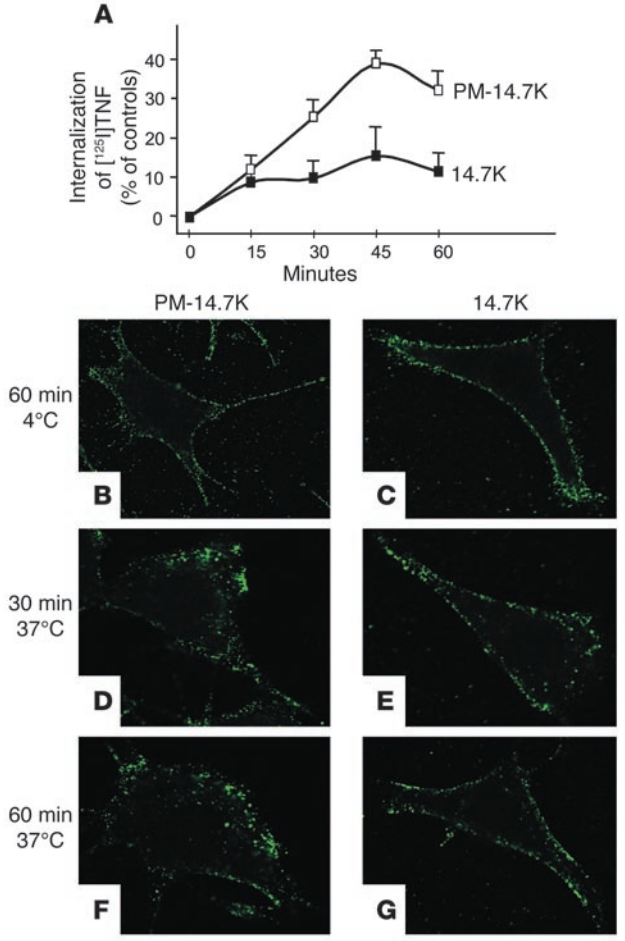

Figure 3
TNFR1 internalization is blocked by 14.7K. (**A**) Internalization of TNFR1 was analyzed in NIH 3T3 cells expressing 14.7K or PM-14.7K by determining the amount of intracellular [^{125}I]TNF at the indicated time points after increasing the temperature to 37°C (mean ± SD; $n = 3$). (**B**–**G**) Confocal laser scanning fluorescence microscopy of TNF receptor distribution on PM-14.7K or 14.7K cells labeled with biotin-TNF/streptavidin-FITC. Labeled TNF receptors were detected after 1 hour at 4°C on the cell surface (**B** and **C**) and intracellularly after 30 and 60 minutes incubation at 37°C in PM-14.7K cells (**D** and **F**). (**E** and **G**) In contrast, labeled TNF receptors remained on the cell surface of 14.7K cells even after 30 and 60 minutes incubation at 37°C, indicating inhibition of TNF receptor endocytosis by 14.7K.

mining the amount of various proteins such as α-adaptin within the isolated magnetic TNFR1 fractions (Figure 2, A and B). Using streptavidin microbeads alone in the absence of biotin-TNF, no TNF receptor–associated proteins were obtained in magnetic preparations, indicating a ligand-specific immunomagnetic preparation of TNF receptosomes and associated proteins (data not shown). Analysis of magnetic TNFR1 fractions from PM-14.7K and 14.7K NIH 3T3 cells revealed recruitment of receptor-interacting protein 1 (RIP-1) and TNF receptor–associated factor 2 (TRAF-2) to the DD of the activated TNFR1 in both cell lines, indicating that in 14.7K cells, the DD is still functional. Interestingly, 14.7K was not found within the isolated magnetic TNFR1 fractions, suggesting little or no direct interactions with proteins at the site of the activated receptor (Figure 2, A and B). As expected according to previous studies, the expression level of PM-14.7K was decreased in comparison to that of 14.7K, probably due to the instability of the mutant protein (19). From these findings, we conclude that 14.7K prevents TNF-induced apoptosis by inhibiting recruitment of TRADD, FADD, and caspase-8 to establish the DISC.

Recently, we identified a distinct domain within the cytoplasmic sequence of TNFR1 responsible for mediating receptor internalization (16). By deleting this endocytic motif, we demonstrated TNFR1 internalization and DISC formation as inseparable events. To investigate the potential interference of 14.7K with TNFR1 endocytosis as a possible reason for inhibition of the DISC formation, we examined TNFR1 internalization by analyzing intracellular accumulation of ^{125}I-labeled TNF. Treatment of PM-14.7K NIH 3T3 cells with ^{125}I-TNF led to a time-dependent increase in intracellular levels of ligand-labeled TNFR1 complexes, which reached a maximum after 45 minutes (Figure 3A). In contrast, a significantly reduced rate of TNFR1 endocytosis was observed in 14.7K NIH 3T3 cells (Figure 3A), indicating a potent inhibition of ligand-activated receptor internalization by 14.7K.

To verify these results, we used confocal microscopy to analyze TNFR1 internalization and subsequent intracellular trafficking in cells treated with biotin-TNF coupled to streptavidin-FITC. PM-14.7K and 14.7K NIH 3T3 cells showed identical staining patterns at the plasma membrane after binding of TNF at 4°C (Figure 3, B and C). After incubation at 37°C for 30 and 60 minutes, labeled TNF was accumulated intracellularly in PM-14.7K cells following TNFR1 endocytosis (Figure 3, D and F). In contrast, nearly all biotin-TNF remained on the cell surface of 14.7K cells after incubation for 30 and 60 minutes at 37°C (Figure 3, E and G). Similar results were obtained with C127 cells (data not shown). These observations were confirmed by analyzing TNFR1 internalization using electron microscopy (Supplemental Figure 1; supplemental material available online with this article; doi:10.1172/JCI23771DS1). In addition, inhibition of TNFR1 internalization by the adenoviral protein 14.7K was found to be specific, as clathrin-mediated internalization of another cell-surface receptor, the transferrin receptor (TfR), did not reveal any obvious differences in TfR endocytosis between PM-14.7K (Supplemental Figure 2A) and 14.7K NIH 3T3 cells (Supplemental Figure 2B). Taken together, these findings clearly demonstrate the selective prevention of TNFR1 endocytosis by 14.7K.

In order to delineate the mechanism of 14.7K-mediated inhibition of TNFR1 internalization, we analyzed receptor endocytosis in more detail. TNFR1 internalization is thought to be mediated by ligand-induced formation of clathrin-coated pits (CCPs) that invaginate to pinch off to become free CCVs (11). The formation of CCPs is induced by the initial recruitment of adaptor protein 2 complex (AP2) to endocytic motifs exposed by activated receptors (24, 25). Clathrin heavy chain was present in all magnetic fractions isolated from both NIH 3T3 and C127 cells expressing PM-14.7K or 14.7K (Figure 4, A–D), ruling out the possibility that clathrin recruitment to the activated TNFR1 was affected by 14.7K expression. The small GTPases Rab4 and Rab5 are endosomal proteins playing important roles in receptor internalization and trafficking via clathrin-CCVs (26, 27). Rab5, which along with Rab4 plays a well-established role in the fusion of endocytic vesicles with endosomes, may be a key regulator for the recruitment of essential

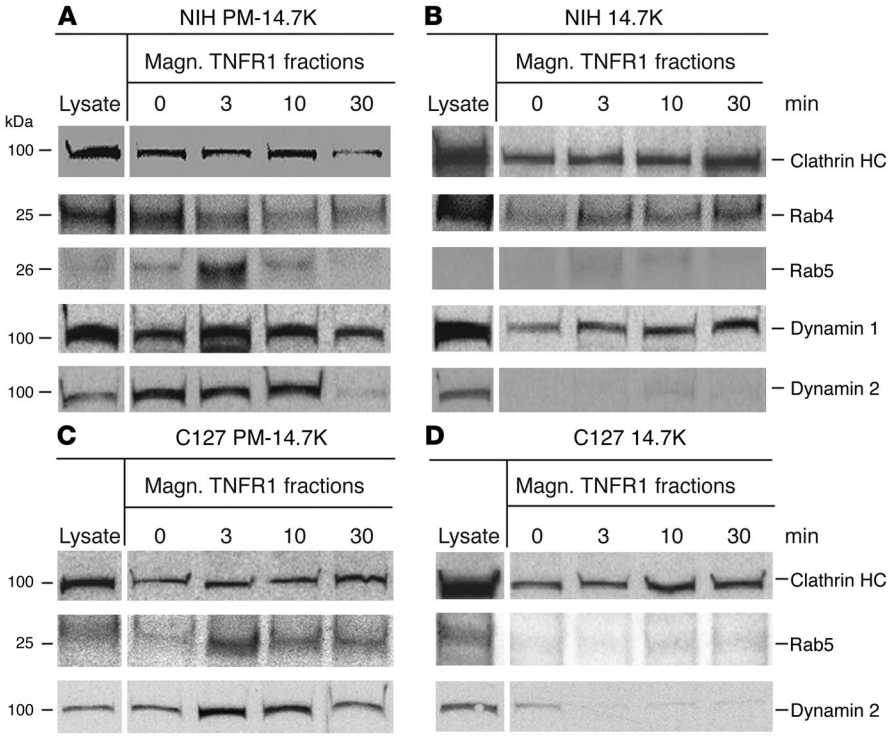

Figure 4
14.7K inhibits recruitment of essential components of the endocytotic machinery. Magnetic TNFR1 fractions were prepared and immunoblotted with the antibodies indicated. Protein cell extracts were used as controls (lysate). NIH 3T3 (**A**) and C127 (**C**) PM-14.7K cells exhibited regular recruitment of the indicated components of the TNFR1-associated endocytotic machinery, while NIH 3T3 (**B**) and C127 (**D**) 14.7K cells lacked Rab5 and dynamin 2.

components of the targeting and fusion machinery for the formation of functional endocytic vesicles (28). To determine the roles of Rab4 and Rab5 in TNFR1 endocytosis, we investigated the occurrence of these Rab proteins in the magnetic TNFR1 fractions. High levels of Rab4 were present in PM-14.7 cells treated with TNF at 4°C (Figure 4A, lane 0 min), which decreased as a result of continuous receptor internalization at 37°C (Figure 4A, lanes 3, 10, and 30 min). Interestingly, Rab5 was associated with the TNFR1 complex only during the first minutes after temperature shift (Figure 4A). In contrast, in 14.7K cells at 4°C (Figure 4B, lane 0 min), Rab4 was found only in minute amounts and accumulated over the next 30 minutes after the temperature was changed to 37°C, but Rab5 was entirely absent (Figure 4B). As the GTPase dynamin is involved in the severing of the neck of CCPs to generate free CCVs (25, 29, 30), we analyzed magnetically labeled TNFR1 complexes for the presence of dynamin 1 and 2. Both isoforms of dynamin were detected in PM-14.7K cells, and their temporal and spatial appearance resembled that of clathrin, indicating generation of free CCVs

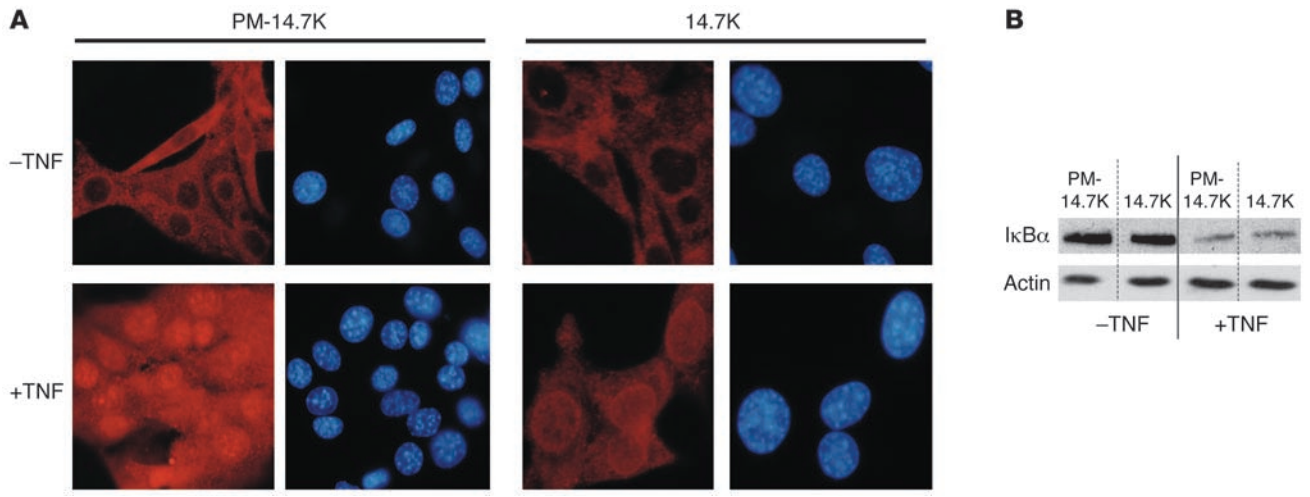

Figure 5
14.7K expression does not affect NF-κB activation. (**A**) NIH 3T3 cells expressing PM-14.7K (left) or 14.7K (right) remained untreated or were treated with 10 ng/ml TNF for 20 minutes, and nuclear translocation of NF-κB was determined by immunofluorescence with an anti–NF-κB antibody (Rhodamine; red). Nuclei were counterstained with Hoechst dye 33258 (blue). (**B**) Cytoplasmic fractions of untreated PM-14.7K and 14.7K NIH 3T3 cells (lanes 1 and 2) or PM-14.7K and 14.7K NIH 3T3 cells (lanes 3 and 4) treated with 10 ng/ml TNF for 20 minutes were prepared and probed for degradation of IκBα. Anti-actin antibody served as a loading control.

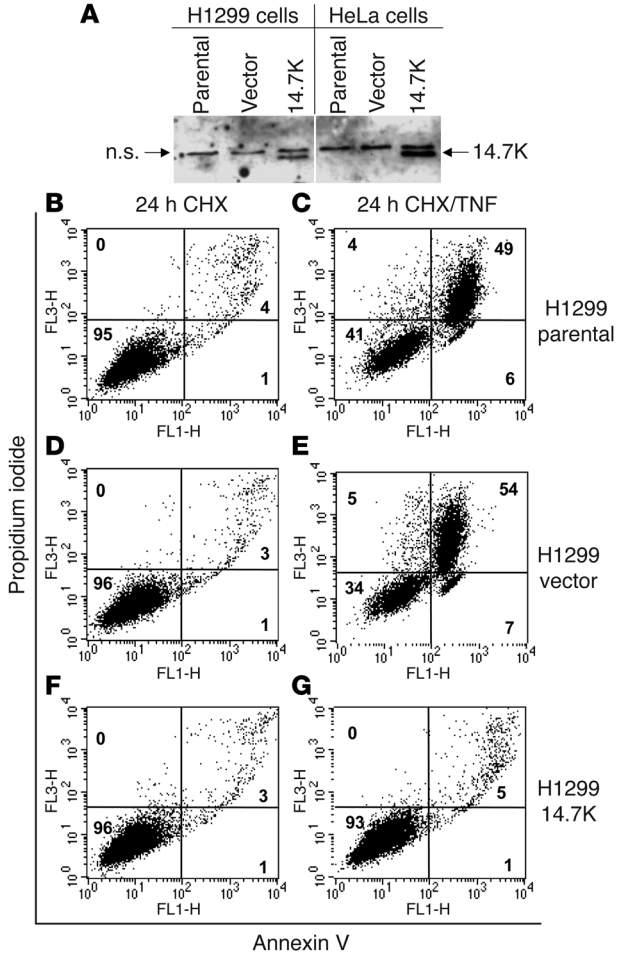

Figure 6
Expression of 14.7K protects human H1299 cells from TNF-induced apoptosis. (**A**) H1299 and HeLa cells were stably transduced with either the empty retroviral vector or a vector encoding 14.7K. Expression of 14.7K protein was confirmed by immunoblotting. n.s., nonspecific. Parental H1299 cells and H1299 cells transduced with empty vector or 14.7K-expressing vector were treated with CHX alone (12.5 μg/ml) (**B**, **D**, and **F**) or TNF (100 ng/ml) plus CHX (12.5 μg/ml) (**C**, **E**, and **G**). Cells were monitored for induction of apoptosis using costaining of FITC–annexin V and propidium iodide detected by FACS analysis.

(Figure 4A). In contrast, dynamin 1 accumulated in 14.7K cells at the site of the activated receptor, whereas dynamin 2 was not detectable (Figure 4B). The lack of Rab5 and dynamin 2 was also observed in magnetic TNFR1 fractions purified from C127 cells. Whereas recruitment of Rab5 and dynamin 2 to TNFR1 was demonstrated in PM-14.7K cells (Figure 4C), both proteins were absent in magnetic fractions from 14.7K cells (Figure 4D). Thus, our data clearly indicate that inhibition of endocytosis by 14.7K is due to a failure in the coordinated temporal and spatial assembly of the essential effector molecules Rab5 and dynamin 2 at the endocytotic machinery of activated TNFR1.

We further investigated the effect of 14.7K-mediated inhibition of TNFR1 internalization on other TNF signaling pathways. Analysis of NF-κB activation revealed rapid TNF-induced nuclear translocation of NF-κB in both PM-14.7K and 14.7K NIH 3T3 cells (Figure 5A) and concomitant proteolytic degradation of cytoplasmic IκBα (Figure 5B). Similar results for NF-κB induction were obtained in C127 cells (data not shown). NF-κB activation is mediated by recruitment of specific adaptor proteins to the DD of TNFR1; accordingly, we observed recruitment of RIP-1 and TRAF-2 to the DD in 14.7K cells (Figure 2). Although some differences were observed concerning the time course and amounts of RIP-1 and TRAF-2 recruitment to TNFR1 (Figure 2), these results clearly demonstrate that 14.7K does not affect NF-κB signaling by targeting TNFR1 internalization.

To date it has been unclear whether expression of the 14.7K protein also protects human cells from TNF-induced apoptosis (4, 31). Therefore, we retrovirally transduced several human cell lines to generate stably transfected cells and analyzed their TNF susceptibility. Expression of 14.7K protein in H1299 and HeLa cells was verified by immunoblotting (Figure 6A). Whereas treatment with CHX alone induced no cytotoxicity in H1299 cells (Figure 6, B, D, and F), TNF treatment of H1299 parental cells and H1299 cells transfected with the empty retroviral vector in the presence of CHX induced apoptosis (Figure 6, C and E). In contrast, H1299 cells expressing 14.7K were completely protected from TNF-mediated cytotoxicity (Figure 6G). Similar results were obtained with HeLa cells (data not shown). From these data we conclude that stable expression of 14.7K can protect different human cell lines from TNF-induced apoptosis in the absence of other adenoviral proteins.

We next tested whether 14.7K-expressing human cells were protected from TNF-induced apoptosis by the same mechanisms as determined in murine cells. TNFR1 internalization was analyzed as before by using biotin-TNF coupled to streptavidin-FITC. After binding of labeled TNF at 4°C for 45 minutes, H1299 parental, H1299 vector, and 14.7K H1299 showed the same staining pattern at the plasma membrane (Figure 7, A–C). After incubation at 37°C for an additional 45–240 minutes, only H1299 parental (Figure 7, D, G, and J) and H1299 vector cells (Figure 7, E, H, and K) displayed TNF-mediated TNFR1 internalization, whereas in 14.7K H1299 cells, the TNF-TNFR1 complexes remained on or near the cell surface (Figure 7, F, I, and L). Similar results were obtained with HeLa cells (Supplemental Figure 3). These results demonstrated that expression of 14.7K can also inhibit TNFR1 internalization in human cells.

To address whether inhibition of TNFR1 endocytosis affects the establishment of the DISC in human cells, we isolated magnetic TNFR1 fractions as described above. After 30 minutes of TNF treatment, TRADD, FADD, and active caspase-8 were detected in magnetic TNFR1 fractions isolated from TNF-susceptible H1299 and H1299 vector cells (Figure 8). TRADD was found to be post-translationally modified by ubiquitinylation (Figure 8 and Supplemental Figure 4), resulting in a form with higher molecular weight, as observed in a previous report (18). In contrast, no recruitment of TRADD, FADD, and active caspase-8 was observed in magnetic TNFR1 fractions purified after 30 minutes from TNF-resistant 14.7K H1299 cells (Figure 8). However, in all cells analyzed, specific recruitment of RIP-1 and TRAF-2 to the DD of TNFR1 was detected after TNF treatment for 30 minutes. This finding indicates that expression of 14.7K selectively interferes with the recruitment of DISC adaptor proteins but does not generally prevent recruitment of other DD-interacting proteins (Figure 8). However, the amount

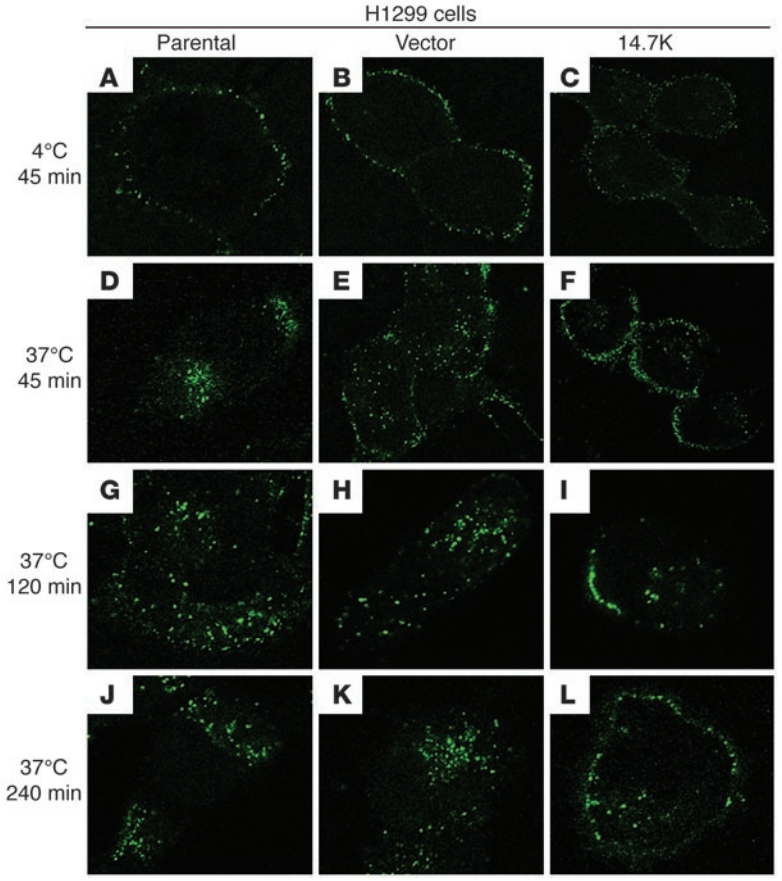

Figure 7

14.7K inhibits TNFR1 internalization in H1299 cells. Cells were labeled with biotin-TNF/streptavidin-FITC complexes at 4°C for 45 minutes (**A**–**C**), and TNFR1 endocytosis was monitored after a temperature shift to 37°C for 45–240 minutes by confocal laser microscopy (**D**–**L**). (**A**–**C**) Labeled TNFR1 complexes were detected after 45 minutes at 4°C strictly on the surface of all cells. After incubation at 37°C for the indicated time points, only in H1299 parental (**D**, **G**, and **J**) and H1299 vector cells (**E**, **H**, and **K**) was TNFR1 endocytosis detected, whereas in 14.7K H1299 cells (**F**, **I**, and **L**), receptor complexes remained on the cell surface, indicating inhibited internalization of TNFR1.

of RIP-1 and TRAF-2 in magnetic TNFR1 fractions from 14.7K H1299 cells was reduced compared with that in fractions from H1299 and H1299 vector cells (Figure 8). In accordance with the above findings in murine cells (see Figure 4), Rab5 and dynamin 2 were absent in magnetic fractions from 14.7K H1299 cells, indicating that expression of 14.7K disturbs the coordinated assembly of the endocytotic machinery at the activated TNFR1 in human cells as well (Figure 8). Identical results were obtained with HeLa cells (Supplemental Figure 5).

Finally, we wanted to evaluate whether the proposed mechanism of 14.7K-mediated TNF resistance in stably transduced murine and human cells is also instrumental in cells infected with wild-type adenovirus. To address this issue adequately, it is necessary to be aware that the adenovirus genome harbors several genes that affect the susceptibility of infected cells to TNF (6, 32, 33). Two E1A-encoded proteins, 289R and 243R, are expressed shortly after cellular uptake of the virus, and the E1A 289R has both transcriptional activation and repression functions (reviewed in ref. 34). Its major biological function for the infection is to push the quiescent epithelial cell into the S-phase of the cell cycle to permit viral DNA synthesis, thereby making the infected cell susceptible to TNF due to accumulation of p53 (35). In contrast, the E1B-19K protein is a viral protein functionally homologous to the antiapoptotic Bcl-2 protein and blocks apoptosis in human cells by interacting with Bax and Bak via its Bcl-2 homology (BH) domain to prevent TNF-induced mitochondrial pore formation (31, 36, 37). In addition, several studies have demonstrated evidence that human cells infected with adenovirus mutants lacking the E1B-19K gene but harboring the entire E3 region were resistant to TNF-induced apoptosis (7, 31). The most likely candidate for mediating this antiapoptotic effect was the 14.7K protein (7, 31).

In order to demonstrate that 14.7K is the only E3-encoded protein able to inhibit TNF apoptosis, we generated 2 adenovirus mutants. One mutant lacks in addition to E1B-19K the entire E3 region (adenovirus 5 [Ad5] 19K$^-$/E3$^-$), and the other mutant lacks E1B-19K but contains the entire E3 region, harboring only a point mutation within the open reading frame of the 14.7K gene (Ad5 19K$^-$/PM-14.7K). This point mutation was shown to completely abolish the protective effect of 14.7K (see Figure 1) (19). In H1299 cells infected with wild-type Ad5 at an MOI of 100, expression of 14.7K was first detectable at 24 hours after infection as determined by immunoblotting (Figure 9A). H1299 cells were then infected with these viruses at an MOI of 100 and treated with TNF, CHX, or CHX and TNF. H1299 cells infected with wild-type adenovirus were completely protected from TNF-induced apoptosis even in the presence of CHX (Figure 9, B and C). Treatment of H1299 cells infected with Ad5 19K$^-$/E3$^-$ mutant with TNF induced apoptosis even in the absence of CHX (Figure 9D). This effect was a direct consequence of expression of E1A 289R protein, which induced TNF susceptibility in virus-infected cells in the absence of TNF-protective proteins (E1B-19K and E3 region) (7, 31). In the presence of TNF and CHX, the apoptotic response in H1299 cells infected with Ad5 19K$^-$/E3$^-$ mutant was even more pronounced (Figure 9E). In addition, infection of H1299 cells with Ad5 19K$^-$/PM-14.7K mutant resulted in TNF-mediated apoptosis when they were treated with TNF alone and TNF plus CHX, as was to be expected due to E1A 289R expression (Figure 9, F and G). These findings clearly demonstrate that in the absence of both E1B-19K and 14.7K, no other E3-encoded protein was able to protect H1299 cells from TNF-mediated apoptosis. Thus, we conclude from our results that expression of 14.7K in wild-type adenovirus–infected human cells can protect from TNF-induced apoptosis.

We next investigated the impact of 14.7K on TNFR1 internalization in adenovirus-infected human cells. As shown in Figure 10, analyses of H1299 cells infected with different adenoviruses revealed a similar membrane staining pattern in all cell lines after incubation with labeled TNF at 4°C, indicating that after 24 hours of infection, TNFR1 was still expressed at the cell surface (Figure 10, A–C). After a temperature shift to 37°C, only in H1299 parental and H1299 vector cells was TNFR1 internalization detected (Figure 10, D and E), whereas in H1299 cells infected with wild-type adenovirus

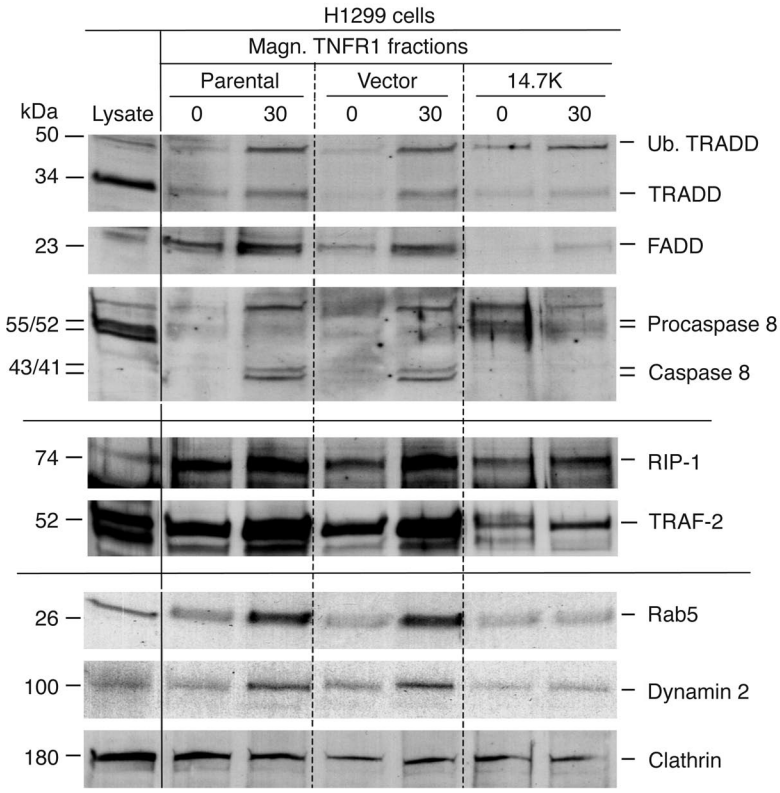

Figure 8
Establishment of the DISC is abolished in magnetic TNFR1 fractions purified from 14.7K H1299 cells. Magnetic TNFR1 fractions were purified from H1299 parental cells and H1299 cells stably transduced with the empty vector or 14.7K gene and immunoblotted with the antibodies indicated. In H1299 parental and H1299 vector cells, recruitment of TRADD, FADD, RIP-1, TRAF-2, and activated caspase-8 was detected after 30 minutes of TNF stimulation. In contrast, in 14.7K H1299 cells, TRADD, FADD, and caspase-8 were not detected after 30 minutes of TNF treatment. The endocytic adaptor proteins Rab5 and dynamin 2 were only recruited to magnetic TNFR1 fractions in TNF-treated H1299 and H1299 vector cells and were absent in preparations from 14.7K H1299 cells. Ub. TRADD, ubiquitinylated TRADD.

expressing 14.7K, TNFR1 endocytosis was inhibited (Figure 10F). These observations demonstrate that during wild-type adenovirus infection, TNFR1 internalization was inhibited due to expression of the 14.7K protein.

In order to study the functional consequences of preventing TNFR1 endocytosis for DISC assembly, we purified magnetic TNFR1 fractions from all virus-infected cell lines. Western blot analysis of the magnetic TNFR1 fractions obtained revealed that in H1299 cells infected with wild-type virus, recruitment of the DISC proteins TRADD, FADD, and active caspase-8 to the DD was nearly completely abolished after TNF stimulation (Figure 11). Because only 85%–95% of all virus-treated cells were infected, as determined from analysis of viral protein expression by immunofluorescence microscopy (data not shown), the minute amounts of TRADD visible in the lane of TNF-treated cells infected with wild-type virus cells were probably due to this inevitable contamination from uninfected cells. In H1299 cells infected with either mutant virus, recruitment of the DISC components was detected in magnetic TNFR1 fractions after 30 minutes, as expected (Figure 11). In addition, in accordance with the results obtained in stably transfected cells, the recruitment of RIP-1 and TRAF-2 to TNFR1 was observed in all cells regardless of the virus used for infection. However, in magnetic fractions isolated from H1299 cells infected with either mutant virus, a slightly enhanced recruitment of RIP-1 and TRAF-2 was observed compared with that in fractions prepared from wild-type virus–infected cells (Figure 11). Furthermore, in accordance with the findings in stably transduced murine and human cells, the recruitment of Rab5 and dynamin 2 to TNFR1 was diminished in wild-type virus–infected cells compared with cells infected with either virus mutant (Figure 11). The small amount of detectable Rab5 and dynamin2 was probably due to inevitable contamination from uninfected cells, as indicated above. Taken together, our results demonstrate that only in wild-type adenovirus–infected cells expressing the 14.7K protein are recruitment of the DISC inhibited and establishment of highly coordinated endocytic machinery at the site of the activated TNFR1 disturbed due to a lack of Rab5 and dynamin 2.

Discussion

This report outlines the retention of TNF-activated TNFR1 at the cell surface as a novel immune escape mechanism for human adenoviruses. The results obtained in this study were derived independently from both murine and human cell lines stably transfected with the viral protein 14.7K in the absence of other adenoviral proteins, as well as from human cells infected with wild-type Ad5 expressing 14.7K. In all 3 experimental approaches, essentially the same 14.7K-mediated mechanism was instrumental for the antiapoptotic effects. The 14.7K protein was found to specifically target assembly of the endocytic machinery to block TNFR1 internalization, causing selective inhibition of recruitment of TRADD, FADD, and caspase-8 to the DD, thereby inhibiting TNF-induced apoptosis. Notably, recruitment of RIP-1 and TRAF-2 to the DD in 14.7K-expressing cells was not significantly affected, indicating that NF-κB activation is not critically dependent on TNFR1 internalization. Thus, the results of this study delineate the molecular mechanism of 14.7K-mediated TNF resistance.

The results of the present study are in perfect agreement with our recently published findings identifying a distinct domain within the cytoplasmic sequence of TNFR1 responsible for mediating receptor endocytosis (16). Expression of an internalization-deficient TNFR1 revealed that receptor endocytosis and DISC formation are inseparable events, thereby demonstrating the

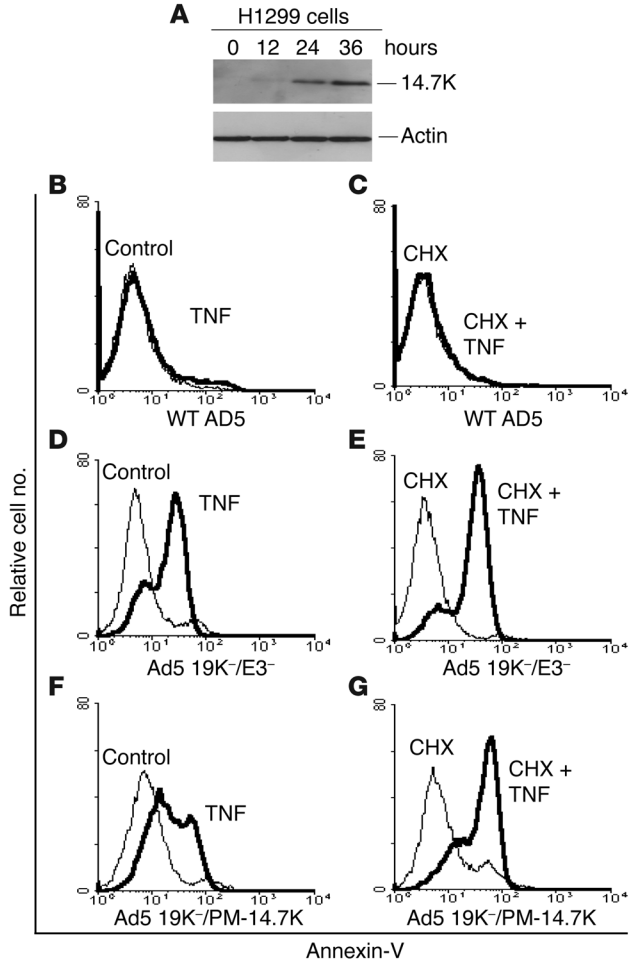

Figure 9
H1299 cells infected with wild-type adenovirus were protected from TNF-induced apoptosis. H1299 parental cells were infected with wild-type adenovirus (WT Ad5) (**A**–**C**) or 2 mutant viruses lacking E1B-19K and the complete E3 region (Ad5 19K⁻/E3⁻) (**D** and **E**) or lacking E1B-19K but containing the complete E3 region, harboring only a point mutation within the 14.7K gene (Ad5 19K⁻/PM-14.7K) (**F** and **G**). (**A**) Expression of the 14.7K protein after infection with wild-type virus was verified by Western blotting. Twenty-four hours after virus infection, the cells were treated with medium as control, TNF, CHX, or CHX plus TNF for 18 hours, and apoptosis was analyzed by flow cytometry. While cells infected with the wild-type Ad5 expressing E1B-19K and 14.7K were completely protected from TNF-induced apoptosis (**B** and **C**), cells infected with the mutant Ad5 19K⁻/E3⁻ were highly susceptible to TNF-induced apoptosis (**D** and **E**) even in the absence of CHX (**D**). (**F** and **G**) Similar results were obtained for cells infected with the mutant Ad5 19K⁻/PM-14.7K.

necessity of TNFR1 internalization for TNF-induced apoptotic signaling. On the other hand, RIP-2 and TRAF-2 were recruited to the DD of internalization-deficient TNFR1, indicating a TRADD-independent recruitment of both adaptor proteins (16). Similar results were obtained in the present study, revealing recruitment of RIP-1 and TRAF-2 to the DD of TNFR1 in cells expressing 14.7K, even though these cells did not form a DISC to mediate apoptosis. Therefore, both studies independently confirm the molecular separation of TNF-induced apoptotic and NF-κB (i.e., antiapoptotic) pathways. The fact that the adenoviral 14.7K protein specifically targets the essential step of TNFR1 internalization in TNF-induced apoptotic signaling underscores the physiological importance of TNF for controlling viral infections (6, 33, 38). Interestingly, the E3 promoter region of human Ad5 contains an NF-κB–binding site, and TNF-treatment enhanced the expression of E3-encoded proteins (39). In a recent study, 14.7K was suggested to potently suppress NF-κB activation in liver homogenates of mice infected with an adenovirus by directly binding to the p50 homodimer (40). In contrast, we did not find any suppression of NF-κB activation in NIH 3T3 and C127 cells expressing 14.7K.

In this study, we used an immunomagnetic purification procedure to isolate intact membrane-enclosed vesicles containing activated TNF receptors and associated adaptor proteins (TNF receptosomes) in a custom-built high-gradient magnetic chamber (16). TNF receptors were labeled with biotinylated TNF and magnetic streptavidin-coated microbeads. Homogenization of TNF-treated cells was performed by a gentle mechanical disruption using glass beads in the absence of detergents, which would have disrupted the

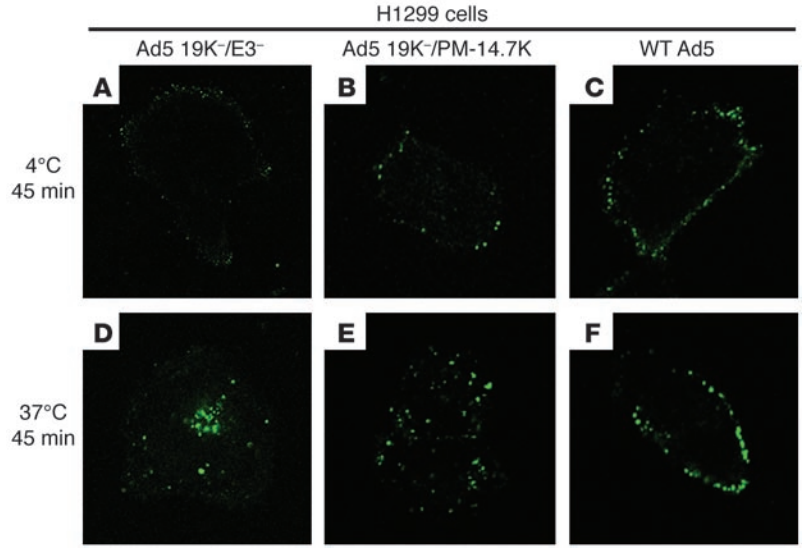

Figure 10
TNFR1 internalization was inhibited in H1299 cells infected with wild-type Ad5. Cells were labeled with biotin-TNF/streptavidin-FITC at 4°C for 45 minutes (**A**–**C**), and TNFR1 endocytosis was monitored after a temperature shift to 37°C for 45 minutes by confocal laser microscopy (**D**–**F**). Only in H1299 cells infected with the mutant Ad5 19K⁻/E3⁻ (**D**) and Ad5 19K⁻/PM-14.7K (**E**) was rapid internalization of labeled TNF-TNFR1 complexes detected, whereas in H1299 cells infected with wild-type Ad5 TNFR1, endocytosis was completely inhibited.

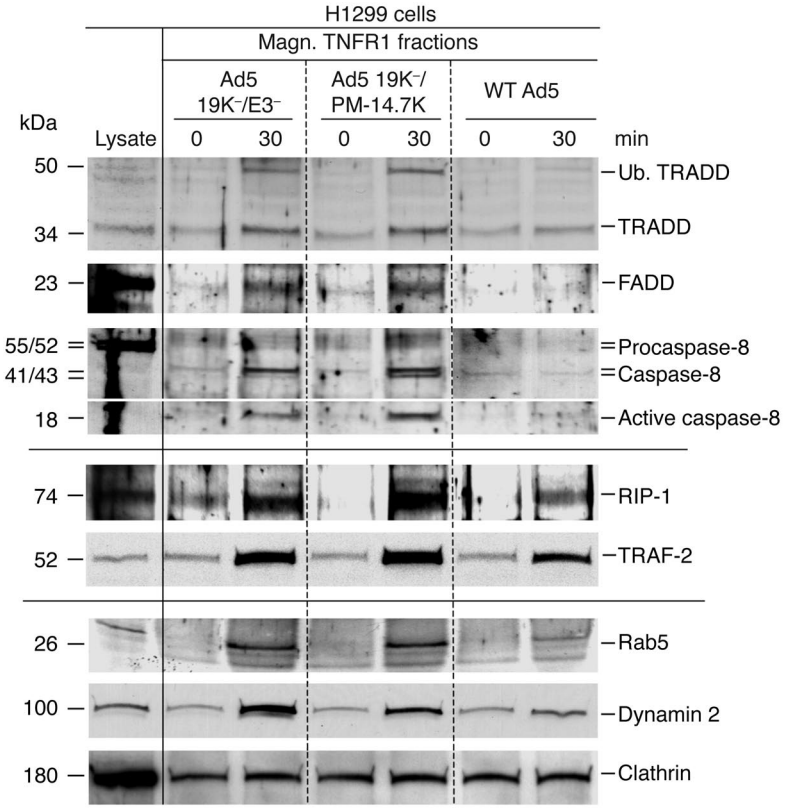

Figure 11
The DISC is absent in H1299 cells infected with wild-type Ad5. Magnetic TNFR1 fractions were prepared from infected H1299 cells and immunoblotted with the indicated antibodies. In H1299 cells infected with the mutant Ad5 19K⁻/E3⁻ and Ad5 19K⁻/PM-14.7K, the DISC proteins TRADD, FADD, activated caspase-8, as well as RIP-1 and TRAF-2 were recruited to TNFR1 after 30 minutes. In contrast, in wild-type Ad5–infected cells, establishment of the DISC was nearly abolished, but RIP-1 and TRAF-2 were still detected. Furthermore, TNF-induced recruitment of the endocytic adaptor proteins Rab5 and dynamin 2 was clearly visible in cells infected with either mutant virus but nearly abolished in cells infected with wild-type virus.

membranes and could have interfered with protein-protein interactions. This immunomagnetic approach was successfully used previously to characterize TNF receptosomes as death-signaling vesicles (16) and to determine the necessity of CD95 internalization for mediating CD95L-induced apoptosis signaling (41).

Inhibition of TNF-induced cytotoxicity by 14.7K was first described in murine cells infected with wild-type group C human adenovirus (7, 8). Furthermore, 14.7K protects cells from TNF-mediated apoptosis by itself in the absence of other viral proteins in stably transfected murine cells lines, without substantially altering cell-surface expression of TNFR1 or TNF affinity (9). In addition, 14.7K expression was found both in the cytoplasm and in the nucleus (8). Furthermore, TNF treatment resulted in an enhanced expression of class I major histocompatibility complex molecules on the cell surface, indicating that 14.7K expression does not alter TNF signal transduction in general (9). Nevertheless, direct evidence that 14.7K protects human cells from TNF-induced apoptosis was still lacking. Our findings that retrovirally transduced 14.7K can protect several human cell lines from TNF-induced cell death by itself in the absence of other adenoviral proteins provides evidence that 14.7K is functional in both murine and human cells. In addition, human cells infected with wild-type adenovirus expressing 14.7K are protected from TNF by the same mechanism instrumental in cells stably transfected with 14.7K, indicating that 14.7K-mediated TNF resistance is a physiologically relevant viral defense to outwit the immune response of the host. A recent report using replication-deficient adenoviruses derived from recombinant E1- and E3-deleted adenoviral vectors suggested that the E3-encoded 10.4K/14.5K heterodimer complex is involved in TNF resistance via downregulation of TNFR1 cell-surface expression (42). In contrast to this, we did not observe internalization of TNFR1 in H1299 cells infected with the wild-type Ad5. In addition, H1299 cells infected with Ad5 19K⁻/PM-14.7K mutant were not protected from TNF-induced apoptosis, although it harbors the complete E3 region including 10.4K and 14.5K but expresses the PM-14.7K protein.

Using replication-deficient recombinant adenoviruses, Chen et al. demonstrated that 14.7K blocks Fas-induced apoptosis and cytolysis induced by transfection of FADD by interacting with caspase-8 (43). However, neither interaction of 14.7K with caspase-8 (44) nor inhibition of Fas-mediated apoptosis was confirmed (45–47).

In order to identify the part of the 14.7K protein essential for mediating the antiapoptotic effect, Ranheim et al. expressed a set of 19 mutants of 14.7K containing various deletions and 6 point mutations, each of which changed a different conserved cysteine residue to a serine (19). Interestingly, the ability of 14.7K to protect against TNF-induced apoptosis was abolished by most of the deletions and single amino acid substitutions, indicating

Table 1
Summary of the genetic status of the viruses used in this study (61)

Virus	E1B-19K	E3 region	Designated in the present study
H5*pg*4156	WT	WT	WT Ad5
H5*pm*4140	Minus[A]	Minus	Ad5 19K⁻/E3⁻
H5*pm*4159	Minus	WT with PM-14.7K	Ad5 19K⁻/PM-14.7K

[A]No protein expression.

the requirement of structural integrity of the whole protein for its proper function (19). In our study, we used one of those mutants with a cysteine residue changed to a serine (C119S) that was shown to completely abolish protection from TNF (19). In accordance with the study mentioned above, we found that this mutant 14.7K (named PM-14.7K in the present study) was expressed at lower levels than the wild-type 14.7K. The early findings that cysteine residues are important for protein stability are in accordance with a recent biophysical study demonstrating that 14.7K binds zinc with a 1:1 stoichiometry (48). Furthermore, the results of that study suggest that 14.7K exists preferentially in a higher-order structure as a nonamer in solution (48).

Another approach used to study the function of 14.7K was the yeast 2 hybrid system to identify potentially interacting proteins (reviewed in ref. 10). The proteins isolated by this method were designated FIPs (14.7K-interacting proteins). FIP1 is a small GTPase interacting with 2 components of the dynein complex, TCTEL (also named GIP-1; GTPase-interacting protein) and GIP-2, both involved in transport of vesicles along microtubules (49, 50, 51). However, there is no experimental evidence that FIP1 is involved in TNF apoptosis signaling. FIP2 is a protein of 577 amino acids containing a Zn finger and 2 leucine zipper domains. 14.7K was shown to interact with its C-terminal Zn finger–binding domain (52). Expression of an N-terminally truncated FIP2 eliminates the protective effect of 14.7K on TNF-induced apoptosis and reverts its subcellular distribution (52). A possible clue for the involvement of 14.7K in the inhibition of intracellular vesicle transport processes may come from the identification of FIP2 binding proteins. Most interestingly, FIP2 interacts with huntingtin, the protein mutated in Huntington chorea that was shown to be part of CCVs, and the GTPase Rab8, regulating the delivery of proteins from the *trans*-Golgi network to the plasma membrane (53). FIP3, also known as NEMO or IKK-γ, is an integral subunit of the IKK complex required for induction of NF-κB activation (54, 55). It was found that coexpression of 14.7K and FIP3 can counteract the localization of FIP3 and apoptosis induction as a result of FIP3 overexpression (54). However, there is no direct evidence linking physiologically expressed FIP3 to TNF-induced apoptotic signaling. FIP4 was identified as apoptosis-inducing factor (AIF), a mitochondrial protein translocating to the nucleus in response to various proapoptotic stimuli (10, 56, 57). To date, the role of FIP4 in 14.7K-mediated TNF resistance remains unclear.

The absence of Rab5 and dynamin 2 from the activated TNF receptor complex provides further evidence for the essential roles these proteins play in TNFR1 endocytosis. Both Rab5 and dynamin are incorporated into CCVs (30, 58), and expression of dominant-negative Rab5a (N34) (58) and dynamin (K44A) (59) results in an abrogation of EGF receptor endocytosis. Because 14.7K is not part of the activated TNF receptor complex, further investigations are needed to address the molecular mechanism enabling 14.7K to selectively interfere with the recruitment of components of the TNFR1-induced endocytotic machinery, such as Rab5 or dynamin 2, while leaving the clathrin-dependent transferrin receptor internalization unaffected.

It is tempting to speculate whether interaction of 14.7K with FIP2 inhibits the proper function of both huntingtin and Rab8 as part of a protein network regulating membrane trafficking and cargo transport of Rab5 or dynamin 2 to the activated TNF receptor complex. Further studies are necessary to decipher the complex interaction of 14.7K with the intracellular vesicle transport network to understand the possible involvement of Rab8 and huntingtin in the TNF-induced apoptosis signaling pathway. Finally, downregulation of other death receptors such as CD95 and TRAIL-R1 and -R2 by the adenovirus E3–encoded 10.4K/14.5K complex was attributed to distinct transport motifs within the viral proteins. These transport motifs mediate ligand-independent internalization and degradation of death receptors (reviewed in ref. 4). Targeting intracellular vesicle transport seems to be an efficient strategy realized by several adenovirus E3–encoded proteins to escape the innate immune response (reviewed in ref. 60).

Methods

Cells and retroviruses. NIH 3T3 and C127 fibroblasts were obtained from the Human Tissue and Tumour Repository of the German Cancer Research Center, Heidelberg, Germany. Packaging cell line GP+E86 and retroviral pLXSN vector were provided by B. Holzmann (Klinikum rechts der Isar, Technical University Munich, Munich, Germany). Wild-type Ad2 DNA was provided by T. Dobner. Retroviral expression inserts were generated by PCR amplification from Ad2 DNA using the following primers: Lex1, 5′-CTCGAATTCATGACTGAATCTCTAGATCTAG-3′ and Lex2, 5′-CTCCTCGAGTTAGTTGAATGGAATAAG-3′ for wild-type Ad2 14.7K; Lex1 and Lex3 (5′-TTAGTTGAATGGAATAAGATCTCTAATACCAGACATGG-3′) were used to generate mutant 14.7K (PM-14.7K) containing a single amino acid exchange at position 119 (C119S) (19). PCR fragments were cloned into the retrovirus vector pLXSN (Clontech; Cambrex), then transfected into the packaging cell line GP+E86 using Lipofectamine reagent (Invitrogen) and selected using G418 (Invitrogen). NIH 3T3 or C127 cells (1×10^5) were infected with supernatants of GP+E86 cells containing the respective recombinant retroviruses and then treated with G418 to remove untransduced cells.

H1299 and HeLa cells were transduced with empty retroviral vector pQCXIP (Clontech; Cambrex) and pQCXIP expressing 14.7K, essentially as described recently (16). After 2–3 rounds of serial transductions, cells were treated with puromycin to eliminate untransduced cells.

Apoptosis assays. For determination of apoptosis, cells were treated with 100 ng/ml TNF for 16–18 hours in the absence or presence of 12.5 μg/ml CHX, then stained with FITC–annexin V (Roche Diagnostics) according to the manufacturer's instructions. Stained cells were analyzed by flow cytometry using a BD FACSCalibur analyzer. Human cells were treated as described above, and apoptosis was determined by flow cytometry after simultaneous staining with FITC–annexin V and propidium iodide (100 ng/ml) (Sigma-Aldrich). Adenovirus-infected H1299 cells were treated with medium as control, CHX, TNF, and TNF in the presence of CHX and stained with FITC–annexin V to determine TNF-induced apoptosis by flow cytometry.

Evaluation of TNF receptor internalization. NIH 3T3 cells expressing 14.7K and PM-14.7K were incubated for 1 hour at 4°C with 1 ng ^{125}I-labeled human recombinant TNF (specific activity, 2,160 kBq/μg; NEN Life Sciences). To allow for TNF receptor internalization, cells were incubated at 37°C for different time periods. The number of intracellular [^{125}I]TNF receptor complexes was determined by passing cells through a pH 3 gradient at 500 *g* consisting of (a) 0.5 ml of culture medium supplemented with 20% Ficoll; (b) 3 ml of 100 mM NaCl, 50 mM glycine-HCl, pH 3, supplemented with 10% Ficoll; and (c) 0.5 ml of culture medium containing 5% Ficoll. The total amount of cell-associated [^{125}I]TNF was determined by replacing the second layer with PBS (pH 7.3) containing 10% Ficoll. Nonspecific binding was assessed by addition of a 200-fold excess of unlabeled TNF. The amount of internalized [^{125}I]TNF at pH 3 was calculated as a percentage of specific binding determined at pH 7.3.

Immunofluorescence analysis of receptor endocytosis. Cells were grown on coverslips in DMEM medium and incubated with 100 ng/ml biotin-TNF (Fluorokine; R&D Systems) for 60 minutes at 4°C. Avidin-FITC reagent was added, and cells were incubated in darkness for another 30 minutes at 4°C. The temperature was shifted to 37°C for the times indicated in the figure legends to allow for receptor internalization. For analysis of TNF receptor endocytosis, cells were fixed with formaldehyde (4% in PBS) for 20 minutes. Cells were analyzed using a Zeiss LSM 510 laser scanning confocal microscope.

Cells were treated with Alexa Fluor 488–labeled transferrin (Molecular Probes; Invitrogen) for 15 minutes at 4°C, then the temperature was increased to 37°C to allow internalization of the transferrin receptor. Reactions were stopped by formaldehyde fixation (4% in PBS) for 20 minutes, and intracellular distribution of transferring receptors was visualized by confocal microscopy at the indicated time points.

Preparation and analysis of magnetic TNFR1 fractions. TNF receptors were magnetically labeled using biotin-TNF (Fluorokine) and 50 nm MACS Streptavidin MicroBeads (Miltenyi Biotec). Cells were incubated in a total volume of 250 μl cold DMEM with 100 μl (400 ng) of biotin-TNF for 1 hour at 4°C, followed by incubation with 200 μl MACS streptavidin microbead solution for 1 hour at 4°C. TNF receptor clustering and formation of magnetized TNF-TNFR1 complexes were achieved by incubation at 37°C for the time periods indicated and stopped by chilling to 4°C. Cells were pelleted by centrifugation at 300 *g* and washed with 0.25 M sucrose buffer, supplemented with 0.015 M HEPES, 100 mg/l $MgCl_2$, pH 7.4, and Protease Inhibitors Set (Roche Diagnostics). Cells underwent gentle, mechanical homogenization with steel beads in 250 μl supplemented sucrose buffer at 4°C, and following centrifugation at 300 *g*, postnuclear supernatant containing intact membrane vesicles was subjected to magnetic separation of TNFR1 fractions in a high-gradient magnetic field. Morphological integrity and purity of the isolated endocytic vesicles harboring labeled TNFR1 were verified by electron microscopy, and TNFR1-associated proteins were separated by SDS-PAGE and analyzed by immunoblotting (16) using antibodies against TRADD (sc-7868; Santa Cruz Biotechnology Inc.), FADD (murine: 7b5, Alexis Biochemicals, Axxora; human: 610399, BD Biosciences), caspase-8 (H134, sc-7890; Santa Cruz Biotechnology Inc.), α-adaptin (M300, sc-10762; Santa Cruz Biotechnology Inc.), clathrin heavy chain (610499; BD Biosciences), Rab 4 (610888; BD Biosciences), Rab5 (KAP-GP006; Biomol International and Stressgen), dynamin 1 (610245; BD Biosciences), dynamin 2 (610263; BD Biosciences), RIP-1 (610458; BD Biosciences), TRAF-2 (C-20, sc-876; Santa Cruz Biotechnology Inc.). Analysis of 14.7K expression in magnetic TNFR1 fractions was done with a polyclonal rabbit anti-14.7K antibody kindly provided by L. Gooding (Emory University School of Medicine, Atlanta, Georgia, USA) and W.S.M. Wold (St. Louis University School of Medicine, St. Louis, Missouri, USA).

Western blotting. Cells were infected with wild-type Ad5 lysed at the indicated time points in 20 mM Tris-HCl pH 7.5, 137 mM NaCl, 0.2 mM EDTA, 1 mM EGTA, 10 mM sodium-β-glycerol-phosphate, 50 mM sodium fluoride, 1% Triton X-100, in the presence of protease inhibitors. Analysis of 14.7K expression was done with a polyclonal rabbit anti-14.7K antibody kindly provided by L. Gooding and W.S.M. Wold using standard methods and visualized by enhanced chemoluminescence (Amersham Biosciences).

NF-κB activation. NIH 3T3 cells were seeded onto chamber slides and were treated with 100 ng/ml TNF for 20 minutes or left untreated, washed with PBS, and fixed with ice-cold ethanol for 10 minutes. NF-κB translocation was determined by staining with anti-p50 NF-κB antibody (Santa Cruz Biotechnology Inc.) and detected with a secondary Cy3-conjugated anti-rabbit antibody (Dianova). Nuclei were counterstained with Hoechst dye 33258 for 5 minutes during the last wash with PBS prior to embedding of the cells.

For analysis of IκBα degradation, 1×10^5 NIH 3T3 cells expressing PM-14.7K or 14.7K seeded in 60-mm cell culture dishes were treated with 10 ng/ml TNF for 20 minutes or left untreated. Cell lysis and immunoblotting using antibodies against IκBα and actin (Santa Cruz Biotechnology Inc.) were done by standard methods and visualized by enhanced chemoluminescence (Amersham Biosciences).

Construction of Ad5 cloning vectors. The adenoviral plasmid pH5*pg*4156 was constructed through multiple rounds of subcloning and modification of restriction endonuclease fragments derived from plasmids pH5*pg*4100 and pFE-1640 (61). The Ad5 genome (35,933 bp) in pH5*pg*4156 is inserted into the *Pac*I site of the bacterial cloning vector pPG-S2 (61). The viral genome is isogenic to the published wild-type Ad5 sequence (GenBank accession number AY339865) and contains a unique endonuclease restriction site at nt 32,834 (*Sfu*I) preceding E4. The Ad5 genome (35,933 bp) in pH5*pg*4156 is inserted into the *Pac*I site of the bacterial cloning vector pPG-S2 (61) and contains 2 additional unique endonuclease restrictions sites at nt 5,764 (*Bst*Z17I) and nt 3,2834 (*Bst*BI) (nucleotide numbering is according to the published Ad5 sequence from GenBank, accession number AY339865). To generate pH5*pg*4156, a 5,827-bp fragment (Ad5 wt nt 27046 to 32872) encompassing E3 was PCR amplified with primers Ad5-E3/Spe (5′-TCAGTAAATACTGCGCGCTGACTCTTAAGGACTAGTTTC-3′) and Ad5-E3/SfuI (5′-GGTGGTGGGGCTATACTACTGAATGAAAAAT-GATTCGAAA-3′) from purified Ad5 *wt*300 DNA and cloned into the *Spe*I/*Sfu*I sites of pH5*pg*4100. The complete sequence of this fragment was determined on both strands by sequence-derived oligonucleotide primers. For the construction of pFE-1640, the 5,827-bp *Spe*I/*Sfu*I fragment was inserted into pPG-S4. The entire sequence of pFE-1640 (7,819 bp) was confirmed by DNA sequencing.

Construction of Ad5 recombinants. To generate Ad5 mutants carrying defined amino acid changes in E1B-19K and 14.7K (Table 1), point mutations were first introduced into the corresponding viral genes in pFE-1640 and pE1-1235 (61) by site-directed mutagenesis with the following oligonucleotide primers: for generation of PM-14.7K: PM-14.7K forward, 5′-CACTCTTATTAAAACCATGTCTGGTATTAGAGATCTTATTCC-3′ and PM-14.7K reverse, 5′-GGAATAAGATCTCTAATACCAGACATGGTTT-TAATAAGAGTG-3′; for generation of mutated E1B-19K: E1B-19K forward, 5′-CCTCATGGAGTGAGAGTGATTGGAAGATTTTTCTGC-3′ and E1B-19K reverse, 5′-GCAGAAAAATCTTCCAATCACTCTCAAGCCTC-CATGAGG-3′. The mutations in these plasmids were verified by DNA sequencing. Finally, the 5,827-bp *Spe*I/*SfuI* or the 7.7-kb *Swa*I/*Bst*Z17I fragment from pH5*pg*4156 was replaced with the corresponding fragments from mutagenized plasmids to generate the adenoviral plasmids listed in Table 1. Recombinant plasmids were partially sequenced to confirm the mutations in the E1B-19K and 14.7K open reading frames. For the generation of virus mutants, the viral genomes were released from the recombinant plasmids by *Pac*I digestion, and viruses were generated exactly as described previously (61). Viral DNA was isolated from viral particles (62) and analyzed by *Hind*III restriction endonuclease digestion. In addition, the viral DNA was partially sequenced to verify the presence of the E1B-19K$^-$ and E3-PM-14.7K mutations.

The following viruses were additionally used in this study. H5*pg*4100 and H5*pm*4140 (61) are isogenic to H5*pg*4156 but lack E3 from nt 28593 to 30471 (Table 1). In addition, H5*pm*4140 contains a nonsense mutation at the seventh codon of the E1B-19K protein coding sequence, which eliminates expression of the E1B-19K product. All viruses were propagated in 293 monolayer cultures. Infections were performed in one-fifth of the normal culture volume in DMEM for 2 hours at 37°C, with gentle rocking every 10 minutes. The virus suspension was then replaced with normal growth medium. The titers of the viruses used in this study were determined by a fluorescent-focus assay as described

previously (61). More detailed information about the cloning and mutagenesis procedures is available in ref. 61.

Virus infections. H1299 cells were seeded the day before infection at a density of 2×10^5 per 60-mm tissue culture disk. After 24 hours, cells were infected with the indicated adenoviruses at an MOI of 100. After an additional 24 hours, cells were treated with medium as control, CHX (12.5 μg/ml), TNF (100 ng/ml), or CHX and TNF, and incubation continued for an additional 18 hours. Monolayers were washed 3 times with PBS, and cells were harvested by incubation in PBS containing 0.02% trypsin (Sigma-Aldrich) and 0.02% EDTA. Cells were pelleted by centrifugation at 300 *g*, washed several times with PBS, and then stained with FITC–annexin V according to the manufacturer's instructions (Roche Diagnostics) to monitor apoptosis induction. To monitor the efficiency of adenovirus infection, we routinely performed analysis of the infected monolayer by immunofluorescence microscopy with an antibody against an E2A-encoded 76-kDa protein, as described previously (61).

Acknowledgments

We thank Andrea Hethke, Friedericke Heiser, Parvin Davania, Maria Kurz, Gertrud Knoll, Sascha Barabas, and Dietmar Gross for excellent technical assistance and Daniela Männel (Institute for Immunology, University of Regensburg) for helpful comments on the manuscript. 14.7K antibodies were kindly provided by Linda Gooding and W.S.M. Wold. The work was supported by grants from the Deutsche Forschungsgemeinschaft (SFB 415 TP A11 and DFG SCHU 733/6-1 to S. Schütze), the Wilhelm-Sander Stiftung (2002.049.1 to S. Schütze and W. Schneider-Brachert), and the Reform B program of the Faculty of Medicine, University of Regensburg (to W. Schneider-Brachert).

Received for publication October 28, 2004, and accepted in revised form August 15, 2006.

Address correspondence to: Stefan Schütze, Institute of Immunology, University Hospital of Schleswig-Holstein, Campus Kiel, Michaelisstr. 5, D-24105 Kiel, Germany. Phone: 49-431-597-3382; Fax: 49-431-597-3335; E-mail: schuetze@immunologie.uni-kiel.de.

Wulf Schneider-Brachert and Vladimir Tchikov contributed equally to this work.

1. Tortorella, D., Gewurz, B.E., Furman, M.H., Schust, D.J., and Ploegh, H.L. 2000. Viral subversion of the immune system. *Annu. Rev. Immunol.* **18**:861–926.
2. Benedict, C.A., Norris, P.S., and Ware, C.F. 2002. To kill or be killed: viral evasion of apoptosis. *Nat. Immunol.* **3**:1013–1018.
3. Fessler, S.P., Delgado-Lopez, F., and Horwitz, M.S. 2004. Mechanisms of E3 modulation of immune and inflammatory responses. *Curr. Top. Microbiol. Immunol.* **273**:113–135.
4. Lichtenstein, D.L., Toth, K., Doronin, K., Tollefson, A.E., and Wold, W.S. 2004. Functions and mechanisms of action of the adenovirus E3 proteins. *Int. Rev. Immunol.* **23**:75–111.
5. Burgert, H.G., et al. 2002. Subversion of host defense mechanisms by adenoviruses. *Curr. Top. Microbiol. Immunol.* **269**:273–318.
6. McNees, A.L., and Gooding, L.R. 2002. Adenoviral inhibitors of apoptotic cell death. *Virus Res.* **88**:87–101.
7. Gooding, L.R., Elmore, L.W., Tollefson, A.E., Brady, H.A., and Wold, W.S. 1988. A 14,700 MW protein from the E3 region of adenovirus inhibits cytolysis by tumor necrosis factor. *Cell.* **53**:341–346.
8. Gooding, L.R., Sofola, I.O., Tollefson, A.E., Duerksen-Hughes, P., and Wold, W.S. 1990. The adenovirus E3-14.7K protein is a general inhibitor of tumor necrosis factor-mediated cytolysis. *J. Immunol.* **145**:3080–3086.
9. Horton, T.M., et al. 1991. Adenovirus E3 14.7K protein functions in the absence of other adenovirus proteins to protect transfected cells from tumor necrosis factor cytolysis. *J. Virol.* **65**:2629–2639.
10. Horwitz, M.S. 2004. Function of adenovirus E3 proteins and their interactions with immunoregulatory cell proteins. *J. Gene Med.* **6**(Suppl. 1):S172–S183.
11. Mosselmans, R., Hepburn, A., Dumont, J.E., Fiers, W., and Galand, P. 1988. Endocytic pathway of recombinant murine tumor necrosis factor in L-929 cells. *J. Immunol.* **141**:3096–3100.
12. Wajant, H., Pfizenmaier, K., and Scheurich, P. 2003. Tumor necrosis factor signaling. *Cell Death Differ.* **10**:45–65.
13. Di Fiore, P.P., and De Camilli, P. 2001. Endocytosis and signaling: an inseparable partnership. *Cell.* **106**:1–4.
14. McPherson, P.S., Kay, B.K., and Hussain, N.K. 2001. Signaling on the endocytic pathway. *Traffic.* **2**:375–384.
15. Schutze, S., et al. 1999. Inhibition of receptor internalization by monodansylcadaverine selectively blocks p55 tumor necrosis factor receptor death domain signaling. *J. Biol. Chem.* **274**:10203–10212.
16. Schneider-Brachert, W., et al. 2004. Compartmentalization of TNF receptor 1 signaling: internalized TNF receptosomes as death signaling vesicles. *Immunity.* **21**:415–428.
17. Harper, N., Hughes, M., MacFarlane, M., and Cohen, G.M. 2003. Fas-associated death domain protein and caspase-8 are not recruited to the tumor necrosis factor receptor 1 signaling complex during tumor necrosis factor-induced apoptosis. *J. Biol. Chem.* **278**:25534–25541.
18. Micheau, O., and Tschopp, J. 2003. Induction of TNF receptor I-mediated apoptosis via two sequential signaling complexes. *Cell.* **114**:181–190.
19. Ranheim, T.S., et al. 1993. Characterization of mutants within the gene for the adenovirus E3 14.7-kilodalton protein which prevents cytolysis by tumor necrosis factor. *J. Virol.* **67**:2159–2167.
20. Chen, G., and Goeddel, D.V. 2002. TNF-R1 signaling: a beautiful pathway. *Science.* **296**:1634–1635.
21. Peter, M.E., and Krammer, P.H. 2003. The CD95(APO-1/Fas) DISC and beyond. *Cell Death Differ.* **10**:26–35.
22. Thorburn, A. 2004. Death receptor-induced cell killing. *Cell. Signal.* **16**:139–144.
23. Barnhart, B.C., and Peter, M.E. 2003. The TNF receptor 1: a split personality complex. *Cell.* **114**:148–150.
24. Collins, B.M., McCoy, A.J., Kent, H.M., Evans, P.R., and Owen, D.J. 2002. Molecular architecture and functional model of the endocytic AP2 complex. *Cell.* **109**:523–535.
25. Marsh, M., and McMahon, H.T. 1999. The structural era of endocytosis. *Science.* **285**:215–220.
26. Ellis, S., and Mellor, H. 2000. Regulation of endocytic traffic by rho family GTPases. *Trends Cell Biol.* **10**:85–88.
27. Rodman, J.S., and Wandinger-Ness, A. 2000. Rab GTPases coordinate endocytosis. *J. Cell Sci.* **113**:183–192.
28. Woodman, P.G. 2000. Biogenesis of the sorting endosome: the role of Rab5. *Traffic.* **1**:695–701.
29. Sever, S. 2002. Dynamin and endocytosis. *Curr. Opin. Cell Biol.* **14**:463–467.
30. Conner, S.D., and Schmid, S.L. 2003. Regulated portals of entry into the cell. *Nature.* **422**:37–44.
31. Gooding, L.R., et al. 1991. The E1B 19,000-molecular-weight protein of group C adenoviruses prevents tumor necrosis factor cytolysis of human cells but not of mouse cells. *J. Virol.* **65**:3083–3094.
32. Schaack, J. 2005. Induction and inhibition of innate inflammatory responses by adenovirus early region proteins. *Viral Immunol.* **18**:79–88.
33. Benedict, C.A., Banks, T.A., and Ware, C.F. 2003. Death and survival: viral regulation of TNF signaling pathways. *Curr. Opin. Immunol.* **15**:59–65.
34. Flint, J., and Shenk, T. 1997. Viral transactivating proteins. *Annu. Rev. Genet.* **31**:177–212.
35. Levine, A.J. 1997. p53, the cellular gatekeeper for growth and division. *Cell.* **88**:323–331.
36. Sundararajan, R., and White, E. 2001. E1B 19K blocks Bax oligomerization and tumor necrosis factor alpha-mediated apoptosis. *J. Virol.* **75**:7506–7516.
37. Sundararajan, R., Cuconati, A., Nelson, D., and White, E. 2001. Tumor necrosis factor-alpha induces Bax-Bak interaction and apoptosis, which is inhibited by adenovirus E1B 19K. *J. Biol. Chem.* **276**:45120–45127.
38. Benedict, C.A., and Ware, C.F. 2001. Virus targeting of the tumor necrosis factor superfamily. *Virology.* **289**:1–5.
39. Korner, H., Fritzsche, U., and Burgert, H.G. 1992. Tumor necrosis factor alpha stimulates expression of adenovirus early region 3 proteins: implications for viral persistence. *Proc. Natl. Acad. Sci. U. S. A.* **89**:11857–11861.
40. Carmody, R.J., Maguschak, K., and Chen, Y.H. 2006. A novel mechanism of nuclear factor-kappaB regulation by adenoviral protein 14.7K. *Immunology.* **117**:188–195.
41. Lee, K.H., et al. 2006. The role of receptor internalization in CD95 signaling. *EMBO J.* **25**:1009–1023.
42. Fessler, S.P., Chin, Y.R., and Horwitz, M.S. 2004. Inhibition of tumor necrosis factor (TNF) signal transduction by the adenovirus group C RID complex involves downregulation of surface levels of TNF receptor 1. *J. Virol.* **78**:13113–13121.
43. Chen, P., Tian, J., Kovesdi, I., and Bruder, J.T. 1998. Interaction of the adenovirus 14.7-kDa protein with FLICE inhibits Fas ligand-induced apoptosis. *J. Biol. Chem.* **273**:5815–5820.
44. Horwitz, M.S. 2001. Adenovirus immunoregulatory genes and their cellular targets. *Virology.* **279**:1–8.
45. Tollefson, A.E., et al. 1998. Forced degradation of Fas inhibits apoptosis in adenovirus-infected cells. *Nature.* **392**:726–730.
46. Shisler, J., Yang, C., Walter, B., Ware, C.F., and Gooding, L.R. 1997. The adenovirus E3-10.4K/14.5K complex mediates loss of cell surface Fas (CD95) and resistance to Fas-induced apoptosis. *J. Virol.* **71**:8299–8306.

47. Elsing, A., and Burgert, H.G. 1998. The adenovirus E3/10.4K-14.5K proteins down-modulate the apoptosis receptor Fas/Apo-1 by inducing its internalization. *Proc. Natl. Acad. Sci. U. S. A.* **95**:10072–10077.
48. Kim, H.J., and Foster, M.P. 2002. Characterization of Ad5 E3-14.7K, an adenoviral inhibitor of apoptosis: structure, oligomeric state, and metal binding. *Protein Sci.* **11**:1117–1128.
49. Li, Y., Kang, J., and Horwitz, M.S. 1997. Interaction of an adenovirus 14.7-kilodalton protein inhibitor of tumor necrosis factor alpha cytolysis with a new member of the GTPase superfamily of signal transducers. *J. Virol.* **71**:1576–1582.
50. Campbell, K.S., Cooper, S., Dessing, M., Yates, S., and Buder, A. 1998. Interaction of p59fyn kinase with the dynein light chain, Tctex-1, and colocalization during cytokinesis. *J. Immunol.* **161**:1728–1737.
51. Lukashok, S.A., Tarassishin, L., Li, Y., and Horwitz, M.S. 2000. An adenovirus inhibitor of tumor necrosis factor alpha-induced apoptosis complexes with dynein and a small GTPase. *J. Virol.* **74**:4705–4709.
52. Li, Y., Kang, J., and Horwitz, M.S. 1998. Interaction of an adenovirus E3 14.7-kilodalton protein with a novel tumor necrosis factor alpha-inducible cellular protein containing leucine zipper domains. *Mol. Cell. Biol.* **18**:1601–1610.
53. Hattula, K., and Peranen, J. 2000. FIP-2, a coiled-coil protein, links Huntingtin to Rab8 and modulates cellular morphogenesis. *Curr. Biol.* **10**:1603–1606.
54. Li, Y., et al. 1999. Identification of a cell protein (FIP-3) as a modulator of NF-kappaB activity and as a target of an adenovirus inhibitor of tumor necrosis factor alpha-induced apoptosis. *Proc. Natl. Acad. Sci. U. S. A.* **96**:1042–1047.
55. Ye, J., Xie, X., Tarassishin, L., and Horwitz, M.S. 2000. Regulation of the NF-kappaB activation pathway by isolated domains of FIP3/IKKgamma, a component of the IkappaB-alpha kinase complex. *J. Biol. Chem.* **275**:9882–9889.
56. Daugas, E., et al. 2000. Apoptosis-inducing factor (AIF): a ubiquitous mitochondrial oxidoreductase involved in apoptosis. *FEBS Lett.* **476**:118–123.
57. Lipton, S.A., and Bossy-Wetzel, E. 2002. Dueling activities of AIF in cell death versus survival: DNA binding and redox activity. *Cell.* **111**:147–150.
58. Barbieri, M.A., et al. 2000. Epidermal growth factor and membrane trafficking. EGF receptor activation of endocytosis requires Rab5a. *J. Cell Biol.* **151**:539–550.
59. Vieira, A.V., Lamaze, C., and Schmid, S.L. 1996. Control of EGF receptor signaling by clathrin-mediated endocytosis. *Science.* **274**:2086–2089.
60. Windheim, M., Hilgendorf, A., and Burgert, H.G. 2004. Immune evasion by adenovirus E3 proteins: exploitation of intracellular trafficking pathways. *Curr. Top. Microbiol. Immunol.* **273**:29–85.
61. Groitl, P., Zeller, T., and Dobner, T. 2006. Construction of adenovirus mutants by direct cloning. In *Adenovirus methods and protocols*. 2nd edition. W.S. Wold, editor. Humana Press. Totowa, New Jersey, USA. In press.
62. Schmid, S., and Hearing, P. 1999. Adenovirus DNA packaging. Construction and analysis of viral mutants. In *Adenovirus methods and protocols*. W.S. Wold, editor. Humana Press. Totowa, New Jersey, USA. 47–59.